

Research Paper

Behavior of Magnetohydrodynamic Waves in the Viscous Coronal Loops

Roza Rezaei¹ · Zahra Fazel^{*2}

¹ Faculty of Physics, University of Tabriz, Tabriz, Iran;
email: rozarezaei72@gmail.com

² Faculty of Physics, University of Tabriz, Tabriz, Iran;
*email: z_fazel@tabrizu.ac.ir

Received: 7 July 2024; Accepted: 24 November 2024; Published: 26 November 2024

Abstract. Studying the dynamics of magnetic plasmas in the presence of pressure gradients, gravity, and Lorentz forces is essential for understanding wave generation and propagation in the solar atmosphere and other magnetic environments. Various solar phenomena, including sunspots, spicules, and coronal loops, are explored within these environments. We consider them as waveguides. These waveguides are interpreted as magnetic flux tubes, providing valuable information about wave properties. The dissipation of magnetohydrodynamic waves in hot coronal loops is investigated using a two-dimensional Cartesian model. The findings demonstrate a decrease in pulse amplitude, and dissipation or damping manifests across distinct segments of the magnetic flux tube as time progresses. We find that the considered viscosity in our model can accelerate the wave damping in the coronal loop, which is in agreement with the results reported by Ofman & Wang (2022).

Keywords: Solar corona, Magnetohydrodynamic waves, coronal loops

1 Introduction

Understanding the sudden increase in the temperature of the sun's corona has been one of the challenges for solar physicists. Aschwanden et al. (2001) emphasized this fact. They applied advanced observations and modeling techniques to understand the complexities of coronal phenomena like loops and eruptions. Their research showed a need for a deeper understanding of the physical processes in the solar corona, especially the mechanism of its unknown heating. Mortel and Hood (2003) concentrated on magnetohydrodynamic (MHD) waves which were potential candidates for energy transport and heating the solar corona. Their investigation indicated how these slow-moving waves propagated through the solar atmosphere and caused them to lose energy. They identified two key damping mechanisms: thermal conductivity, which transferred heat within the coronal plasma, and compressive viscosity, which revealed the plasma's resistance to pressure changes and deformation. Their studies specifically focused on the "thermal" mode of MHD waves, which was only active in the presence of thermal conductivity. They applied it in stationary thermal waves, damping occurred as energy dissipation, meaning the waves continuously lost their energy. However,

* Corresponding author

This is an open access article under the CC BY license.



the damping occurred oscillatory in driven waves. This showed a complex interaction between wave propagation and thermal conduction. Furthermore, Mortel and Hood realized that higher thermal conductivity caused slower wave propagation and energy dissipation. They calculated the minimum time required for complete wave energy dissipation through thermal conductivity. Finally, by comparing their simulations with spacecraft observations, they concluded that thermal conductivity was probably the main mechanism for damping slow MHD waves [1,2]. Nakariakov and Verwichte (2005) investigated coronal waves and oscillations in the solar corona. They applied advanced imaging cameras and spectroscopic instruments across various wavelengths, including visible light, ultraviolet, X-rays, and radio waves. They focused on analyzing these waves within the magnetohydrodynamic (MHD) wave theory framework. They concluded that modeling interactions of MHD waves with solar plasma helped identify different wave types, and these waves were applied for remote detection and a better understanding of the physical properties and structure of the solar corona [3].

Kumar et al. (2006) researched the heating of the solar corona using magnetohydrodynamic waves. The results indicated that waves in dense plasma with a low β parameter were divided into three modes: slow, fast, and thermal. Slow waves could contribute to the heating of the solar corona, while fast waves could affect active regions of the Sun [4]. Gruszkowski et al. (2011) investigated the fast magneto-acoustic waves in magnetic loops. They applied a two-dimensional box model of coronal loops without considering the effects of gravity and magnetic curvature. Their results demonstrated that fast magneto-acoustic waves were generated throughout the magnetic field, and with an increase in plasma β , the speed of these waves increased [5]. Murawski et al. (2012) investigated magneto-acoustic oscillations in the solar corona. They examined the effect of shock waves on these oscillations using computer simulations. They concluded that shock waves could excite oscillations with periods of several minutes in the corona. The period of these oscillations depended on the depth and intensity of the shock waves [6]. Mandal et al. (2016) studied slow magneto-acoustic waves in hot solar coronal loops. They applied the X-ray telescope (XRT) and the Atmospheric Imaging Assembly (AIA) of the Solar Dynamics Observatory (SDO) to observe these waves. They concluded that these waves appeared after the occurrence of a microflare in the loops and propagated at the local sound speed. As they moved along the loop, the amplitude of their intensity perturbations decreased, and ultimately they vanished [7].

Studies on magneto-hydrodynamic (MHD) waves in coronal loops offered valuable insights into the physical properties of the solar corona. Nakariakov et al. (2020) investigated the effect of coronal loop length on the period of "kink oscillations," a specific type of wave motion. They further demonstrated that the damping of both "kink" and "slow" oscillations depended on their magnitude, highlighting the significance of nonlinear damping mechanisms. This information was crucial for analyzing key parameters of coronal plasma, such as Alfvén speed, magnetic field structure, stratification, temperature, and the fine details of its structure [8]. For instance, Fathalian and Safari (2010) investigated the effects of longitudinal density stratification along the loop axis on the collective kink-like modes of coronal loop systems. They modeled the coronal loop system as cylinders of parallel flux tubes with two ends of each loop which they related to the higher density of the photosphere. They investigated the effect of the stratification on the frequencies and frequency ratios within the coronal loop systems. Their studies showed that the increasing longitudinal density stratification parameter caused an increase in frequencies. The results indicated that frequency ratios in coronal loop systems were sensitive to the density scale height parameter, and density stratification should be considered in the dynamic analysis of coronal loop systems. Based on this knowledge and considering compressive viscosity, Ofman and Wang (2022) investigated the excitation and propagation of magneto-acoustic waves in hot coronal

loops. They constructed the 3D MHD models using real solar images and investigated how magnetic field geometry, temperature variations, and increasing density within the loops influenced wave behavior. In their model, they examined the role of compressive viscosity, which could induce wave propagation along magnetic field lines. The results indicated that compressive viscosity positively influenced interactions between various types of waves in hot coronal loops [9,10].

In this paper, we investigate the behavior of magnetohydrodynamic (MHD) waves in viscous coronal loops using a two-dimensional Cartesian model and numerical simulations. Based on the foundational work of Ofman and Wang (2022) which examined the role of compressive viscosity in wave propagation, our research demonstrated that viscosity and density variations at different heights lead to a decrease in the amplitudes of the velocity field oscillations. In this work, Section 2 presents the basic equations, theoretical model and initial condition. In Section 3 we present the results and finally, Section 4 is devoted to the discussion and conclusion.

2 Theoretical model

To investigate wave dissipation, we use magnetohydrodynamic equations in a two-dimensional Cartesian model on the (x, z) plane. The effect of magnetic diffusion is neglected, and the plasma flow is assumed to be incompressible. The fundamental equations are as follows [11]

$$\frac{\partial \vec{B}}{\partial t} = \nabla \times (\vec{V} \times \vec{B}), \quad (1)$$

$$\rho \frac{\partial \vec{V}}{\partial t} + \rho (\vec{V} \cdot \nabla \vec{V}) = -\nabla p + \rho \vec{g} + \vec{J} \times \vec{B} + \rho \nu \nabla^2 \vec{V}. \quad (2)$$

After linearization, we have the dimensionless equations

$$\frac{\partial \bar{B}_y}{\partial \bar{t}} = \bar{B}_0 \frac{\partial \bar{V}_y}{\partial \bar{z}} - \bar{V}_0 \frac{\partial \bar{B}_y}{\partial \bar{z}}, \quad (3)$$

$$\bar{\rho}_0 \frac{\partial \bar{V}_y}{\partial \bar{t}} + \bar{\rho}_0 \bar{V}_0 \frac{\partial \bar{V}_y}{\partial \bar{z}} = -\frac{1}{\bar{\rho}_0} \left(\frac{\partial P_1}{\partial z} \right) + \frac{1}{\bar{\rho}_0} \mathbf{B}_0 \frac{\partial \bar{B}_y}{\partial \bar{z}} + \bar{\rho}_0 \nu \nabla^2 \bar{V}_y. \quad (4)$$

The initial equilibrium of the system, which has not yet been perturbed, is defined by the following equations: initial velocity, initial magnetic field, and initial density of the tube.

$$\vec{V}_0 = V_0 \hat{k}, \quad (5)$$

V_0 is the initial velocity of the plasma flow, assumed to be uniform along the axis of the flux tube.

$$\vec{B}_0 = B_0 \hat{k}, \quad (6)$$

it is the initial magnetic field of the system, chosen to be uniform along the z -axis

$$\rho_0(z) = (\alpha + \text{tgh}(\alpha(z-1)))^{-2}. \quad (7)$$

The initial density of the system depends on the height or length of the chosen tube, which is considered as a hyperbolic tangent of α (where $\alpha=2$ controls the inhomogeneity across the magnetic field). Density changes occur along the tube and the z -axis, leading to stratification effects. The impact of stratification gradually decreases. In the equation of motion, viscosity and density oscillations with height introduce a damping effect on waves moving through

the system.

For the perturbed velocity, we consider the following profile (Figure 1)

$$V_y(x, z, t = 0) = A_v \exp\left(-\frac{(x - x_0)^2 + (z - z_0)^2}{w^2}\right), \quad (8)$$

$A_v = 2$ km/s is the amplitude of the initial Gaussian pulse. $z_0 = 0$ and $x_0 = 1$ are the initial positions, and w is the width of the pulse. We set and hold fixed, $w = 0.5$ Mm.

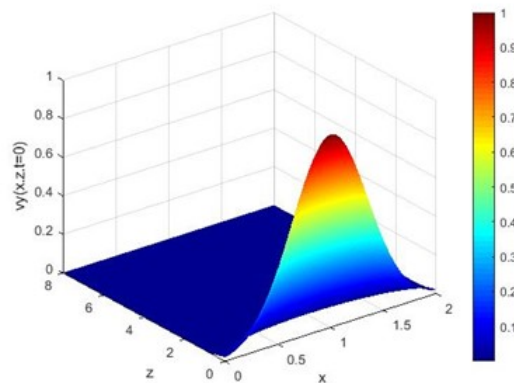


Figure 1: Spatial variation of the V_y , perturbed velocity in X-Z space at $t = 0$.

3 Results

We solved the time and spatial derivatives in equations (3) and (4) and applied numerical methods. We employed the fourth-order Runge-Kutta method and the finite difference scheme. The simulation box consists of 256×256 grid points, or 65536 points in all. The total simulation period is set to $T = 18$ (dimensionless time), which is the final time in the simulation code. The time step is chosen as 0.001. By multiplying the dimensionless time values by a time scale ($\tau = 2.2$ min), they can be expressed in minutes. The simulated box length is adjusted in dimensions (x, z) and assumed to be (2, 8). The assumed flux tube space is given as 2000 km (coronal loop diameter) and 10000 km (loop height). The value of the viscosity coefficient is considered about $\nu_0 \sim 7.6 \times 10^{-5}$, which is for the coronal conditions [10].

4 Conclusion

To investigate the behavior of waves propagating in the flux tube, we first introduced a perturbation by introducing an initial velocity pulse into the system. Over time, the perturbed velocity field began to propagate. Due to the presence of dissipative agents such as viscosity and the density stratification, the amplitude of oscillations decreased at different points in the simulated box. The obtained results were plotted as graphs showing the changes in the perturbed velocity field of the system, both spatially and temporally. In the graphs, temporal changes in the perturbed velocity for different positions of the flux tube are observed with consistent damping and a noticeable decrease in amplitude. In Figure 2, since

the initial pulse has a width, it takes about (1-1.5) dimensionless time for the pulse to pass. After the pulse passes, the oscillations created behind it undergo gradual amplitude decay with time; it depends on the conditions of the pulse tube. As can be seen from the graph, the pulse and its perturbation pass through the region ($z = 1$), and damping is observed in them. After a time of ($t = 2.2$), the pulse reaches a height of $z = 4$ (Figure 3). Due to changes in density with height, the pulse propagates with a damping speed. The graph shows a decrease in the amplitude over time at the higher elevations of the tube.

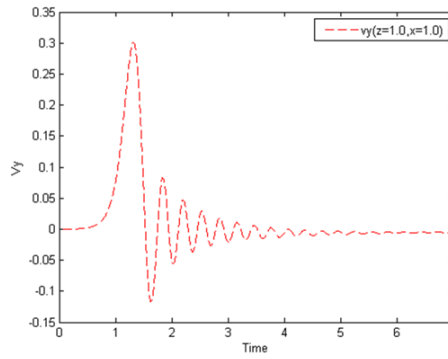


Figure 2: Spatial variation at $Z = 1$ (bottom of the simulated box).

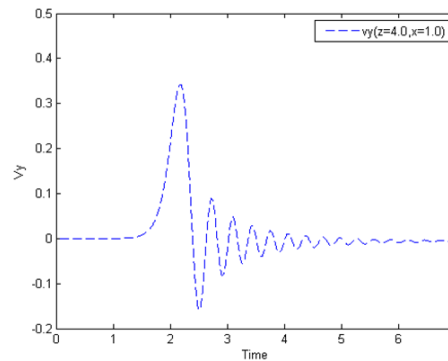


Figure 3: Spatial variation at $Z = 4$ (middle of the simulated box).

In Figure 4, at a height of $z = 7.65$, which is close to the boundary, the pulse starts to oscillate at around time ($t = 6$) and passes at time ($t = 7.6$). The effects of the pulse will continue until time $t = 10$. The amplitude of the pulses changes significantly during propagation. By comparing the propagation of pulses in the three graphs above, we can conclude that the width and amplitude of the pulses change gradually as they move along the z -axis of the tube, but there is a noticeable decrease in amplitude over time at each height of the tube. Our findings demonstrate that there is a decrease in pulse amplitude and the dissipation manifests across distinct segments of the magnetic flux tube as time progresses. From our model, we find that the viscosity plays an important role in propagation of the waves and it can accelerate the wave damping in the coronal loop. This result is in good agreement with the results of Wang (2011), Kumar et al. (2015) and Ofman & Wang (2022)

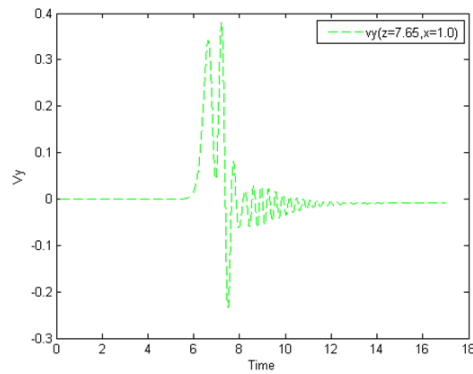


Figure 4: Temporal variation of the perturbed velocity V_y in situation $Z = 7.65$ (top of the simulated box).

[10,12,13].

Authors' Contributions

All authors have the same contribution.

Data Availability

The data that support the findings of this study are available from the corresponding author upon reasonable request.

Conflicts of Interest

The authors declare no potential conflicts of interest.

Ethical Considerations

The authors have diligently addressed ethical concerns, such as informed consent, plagiarism, data fabrication, misconduct, falsification, double publication, redundancy, submission, and other related matters.

Funding

This research did not receive any grant from funding agencies in the public, commercial, or nonprofit sectors.

References

- [1] Aschwanden, M. J., & Poland, A. I., 2001, ARA&A, 39, 175.

- [2] De Moortel, I., & Hood, A. W., 2003, *A&A*, 408, 755.
- [3] Nakariakov, V. M., & Verwichte, E., 2005, *Living Rev. Solar Physics*, 2, 3.
- [4] Kumar, N., Kumar, P., & Singh, S., 2006, *A&A*, 453, 1067.
- [5] Gruszecki, M., & Nakariakov, V. M., 2011, *A&A*, 536, 68.
- [6] Konkol, P., Murawski, & K., Zaqarashvili, T. V., 2012, *A&A*, 537, 96.
- [7] Mandal, S., Yuan, D., Fang, X., & et al., 2016, *ApJ*, 828, 72.
- [8] Nakariakov, V. M., & Kolotkov, D. Y., 2020, *ARA&A*, 58, 441.
- [9] Fathalian, N., & Safari, H., 2010, *ApJ*, 724, 411.
- [10] Ofman, L., & Wang, T. 2022, *ApJ*, 926, 64.
- [11] Priest, E., 1982, *Magnetohydrodynamics of the Sun.*, 86.
- [12] Wang, T., 2011, *SSRV*, 158, 397.
- [13] Kumar, P., Nakariakov, V. M., & Cho, K. S., 2015, *ApJ*, 804, 4.